euspen's 20th International Conference & Exhibition, Geneva, CH, June 2020
www.euspen.eu

Influence of the accuracy between thin-walled fixture and parts in ultra-precision grinding

Lai Hu[1], Jun Zha[1], Yaolong Chen[1]

[1]*School of Mechanical Engineering, Xi'an Jiaotong University, Xi'an 710049, China*

jun_zha@xjtu.edu.cn

Abstract
The influence between fixture and part accuracy in ultra-precision grinding of thin-walled parts was researched in this paper. Two different types of thin-walled parts (Diameter/length = 1:20 and 20:1) were analysed. Firstly, based on the theory of small displacement torque (SDT), the influence on the machining accuracy of thin-wall fixtures and parts was deduced theoretically. A set of theoretical models for accuracy prediction are established. It can be found that the error value is very large during the first grinding. At the same time, within a certain grinding time, the error becomes smaller and smaller. The first maximum error is 0.066 mm and the fourth maximum error is 0.008 mm. After that, an ultra-precision machining experiment was carried out to verify the generality of the method. The results show that the final test accuracy deviation is within the range of 2% under two different machining processes.

ultra-precision machining; Thin-walled parts; fixture

1. Introduction

The application of high-speed and ultra-high-speed ultra-precision machining is becoming more and more important in industrial production. The machining accuracy of machine tools is one of the important factors that determine the accuracy of parts [1-2]. At the same time, in parts manufacturing, thin-wall parts processing is the difficulty and focus in the processing field. For the manufacture of thin-walled parts, many researchers and workers have designed the corresponding tools and fixtures to avoid or reduce the deformation and precision influence in the processes. Many authors have also made other related researches on methods to reduce workpiece errors. For example, Huan et al [3] proposed a method of graphic display and evaluation. The display and evaluation software module of CNC non-circular grinder controller is developed and integrated into CNC non-circular grinder controller. Fu et al [4] proposed a geometric error compensation method for numerical control machine tools based on workpiece model correction and numerical solution of equations. However, most precise machine tools have errors, plus repeated errors such as tooling and fixture errors and parts manufacturing. The error of the final manufactured parts will be even greater. However, the error between the fixture and the part and the error affecting the final machining accuracy of the part can be controlled. Therefore, the focus of this paper is to obtain the measurement accuracy and measurement error at different times through the actual thin-walled parts processing test for theorization. A theoretical model is formed based on the errors of tooling and fixture and machined parts in the process of thin-wall ultra-precision machining.

2. Accuracy Analysis of Tooling and Fixture for Thin-walled Parts

The analysis of the theoretical model is mainly based on the actual processing of thin-walled parts (diameter/length=20:1). The entity is first machined by a thin-walled part as shown in Figure 1.

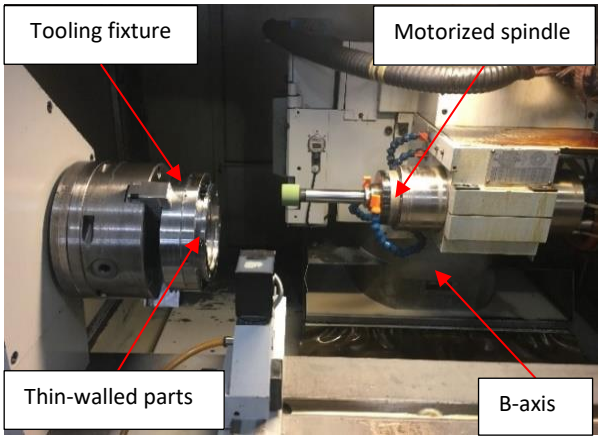

Figure 1. Physical drawing of thin-wall parts

Actual experiments and on-site phased precision tests of machined parts are carried out. The grinding processes repeated four times, and tested three times after each circle. The test method is to use dial gauge to test the straight run-out of the outer circle and the straight run-out of the end face. At the same time, the full runout of the outer circle and the full runout of the end face are tested. Both the 0-1 and 1-2 have grinding depth 0.1 mm, for 2-3 and 3-4 are 0.3 mm and

0.7 mm, respectively. The four times accuracy test curves are shown in Figure 2.

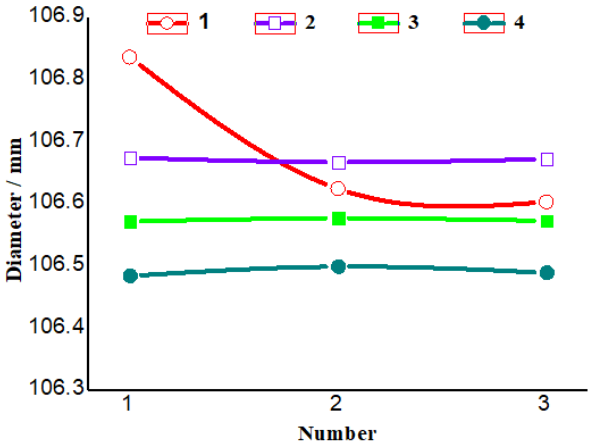

Figure 2. Accuracy curves of four different test

As shown in Figure 2, the accuracy error of the three tests after the first grinding test is the largest. The test accuracy after the second, third and fourth grinding is basically the same. It can be analysed that there are many reasons for the large error of the first precision, but the most important factor is that the precision of the tooling fixture and the matching precision of the tooling fixture and the processed parts have the greatest influence [5]. Therefore, this part should be analysed theoretically.

3. Mapping relation of SDT theoretical model

The thin-walled parts, tooling fixtures and thin-walled test pieces will be separately extracted for analysis. The assembly simplification is shown in Figure 3.

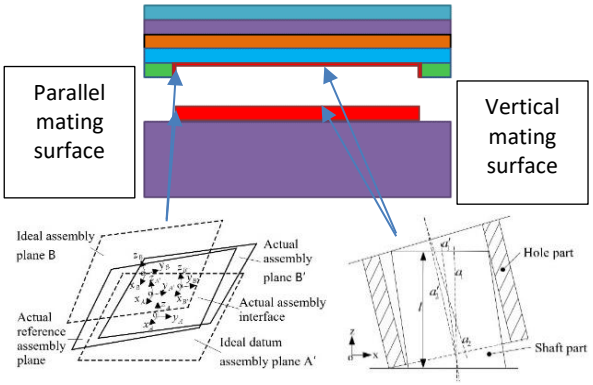

Figure 3. Simplified diagram of fixture matching with thin-wall parts

As shown in figure 3, the crimson part is the mating surface. It can be seen that the matching part has roundness matching and plane matching, the tooling fixture is the reference part, and the workpiece is the assembled part. Therefore, theoretical modelling and analysis are proposed for this kind of matching accuracy working condition.

Assume that the two planes are A and B respectively. The error variation matrix of the joint surface from plane to plane can be expressed as follow,

$$M_{AB}=\begin{bmatrix} 1 & -\delta_{AB} & \beta_{AB} & u_{AB} \\ \delta_{AB} & 1 & -\alpha_{AB} & v_{AB} \\ -\beta_{AB} & \alpha_{AB} & 1 & w_{AB} \\ 0 & 0 & 0 & 1 \end{bmatrix} \quad (1)$$

In Eq.1, α_{AB}, β_{AB} and δ_{AB} represent the error components of the plane rotating about the *x*, *y*, z axis relative to the plane A, respectively. u_{AB}, v_{AB} and w_{AB} represent the error components of plane B in translation along the *x, y, z* axis relative to plane A, respectively. According to the error formation process, Eq.3 can be expressed as follow,

$$M_{AB}=M_{AA'}\times M_{A'B'}\times M_{B'B} \quad (2)$$

Where $M_{AA'}$, $M_{A'B'}$ and $M_{B'B}$ represents the error variation matrix from the ideal reference assembly plane A to the actual reference assembly plane A' and the error variation matrix from the actual reference assembly plane A' to the actual assembly plane B' respectively, and the error variation matrix from the actual assembly plane B' to the ideal assembly plane B.

Similarly, the variation of error components of each part of the cylindrical joint surface is as follow,

$$\begin{cases} \beta_{iL}\le\beta_i\le\beta_{iU} \\ u_{iL}\le u_i\le u_{iU} \\ u_{iL}\le u_i+z\cdot\beta_i\le u_{iU} \end{cases} \quad (i=11',1'2',2'2) \quad (3)$$

In Eq.3, 11', 1'2' and 2'2 corresponding to *i* respectively represents from the ideal axis to the actual axis, the actual axis of the axis to the actual axis of the hole, and the actual axis of the hole to the ideal axis. β_{iu} and β_{iL} are that upper limit value and the low limit value of the variation interval of the error component β of the part i respectively; u_{iU} and u_{iL} are the upper limit value and the lower limit value of the variation interval of the error component *u* of the *i* part respectively, -l/2≤Z≤l/2. The error of the cylinder joint surface is,

$$\begin{cases} \beta_{12}=\beta_{11'}+\beta_{1'2'}+\beta_{2'2} \\ u_{12}=u_{11'}+u_{1'2'}+u_{2'2} \end{cases} \quad (4)$$

Combining Eq.3 and 4, the variation interval of each error component of the cylindrical joint surface can be obtained, and the error variation matrix of the cylindrical joint surface is as follow,

$$M_{12}=\begin{bmatrix} 1 & 0 & \beta_{12} & u_{12} \\ 0 & 1 & -\alpha_{12} & v_{12} \\ -\beta_{12} & \alpha_{12} & 1 & 0 \\ 0 & 0 & 0 & 1 \end{bmatrix} \quad (5)$$

Where, β_{12} and u_{12} can be solved according to Eq.5, and α_{12} and v_{12} can be solved through the relationship with β_{12} and u_{12} or a solution process similar to β_{12} and u_{12}.

Combining the plane error variation matrix and the cylinder error variation matrix, the derivation is as follow,

$$M_{F(x)}=M_{AB}\times M_{12}=M_{AA'}\times M_{A'B'}\times M_{B'B}\times M_{12} \quad (6)$$

In Eq.6, $M_{F(x)}$ corresponds to the total error variation matrix function of the combination of the plane error variation matrix and the cylindrical error variation matrix. Simultaneously, considering both the weight of plane error variation matrix M_{AB} and cylindrical error variation matrix M_{12} are 1. This is the representation of the false weight listed for the plane error variation matrix and the cylindrical error variation matrix. In this way, the total weight values of the two errors can be finally obtained. The purpose of analysing the total weight value is to obtain whether the error of the machined parts based on this clamping method meet the actual requirement, and to find out which of the two errors

will have greater influence, and to obtain the trend of error range at the same time.

In order to explain the advantages of this theoretical model, the data previously processed and measured are analysed. The SDT theoretical operation is carried out, and the results are as follow,

$$M_{F(1)} = \begin{bmatrix} 1 & 0 & 0.066 & 0.084 \\ 0 & 1 & -0.063 & 0.084 \\ -0.066 & 0.063 & 1 & 0 \\ 0 & 0 & 0 & 1 \end{bmatrix}$$

$$M_{F(4)} = \begin{bmatrix} 1 & 0 & 0.008 & 0.002 \\ 0 & 1 & -0.006 & 0.002 \\ -0.008 & 0.006 & 1 & 0 \\ 0 & 0 & 0 & 1 \end{bmatrix} \quad (7)$$

In Eq.7, the error values measured for the first grinding and the third grinding are very large, and the error will become smaller and smaller when grinding tests are carried out continuously. The first maximum error is 0.066 mm, and the fourth maximum error is only 0.008 mm. It shows that there is an adaptive process in the matching accuracy between the tooling fixture and the machined parts during the continuous machining process. In the same way, another thin-walled part (length/diameter=20:1) is verified and tested by a precision three-coordinate measuring instrument with accuracy 0.3+L/1000μm (*L* is the measurement length, mm). Another part processing is shown in Figure 4. The test results are shown in Table 1 and the test data are shown in Figure 5.

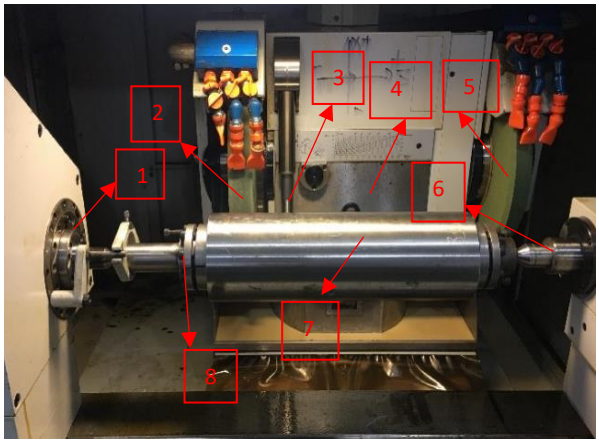

Figure 4. Machining Site of Motorized Spindle part
1 Workpiece C axis; 2 Cylindrical grinding wheel; 3 ruby probe; 4 Axis B; 5 30 ° end face grinding wheel; 6 tailstock; 7 Motorized spindle part; 8 tooling fixture

Table 1. Test results of part (length/diameter=20:1)

Test Items	Error/mm	Test Items	Error/mm
Internal bore surface 1	0.0201	Internal bore surface 2	0.0158
Inner bore surface 1	0.0195	Inner bore surface 2	0.0116
Inner bore surface 1	0.0056	Inner bore surface 2	0.0055

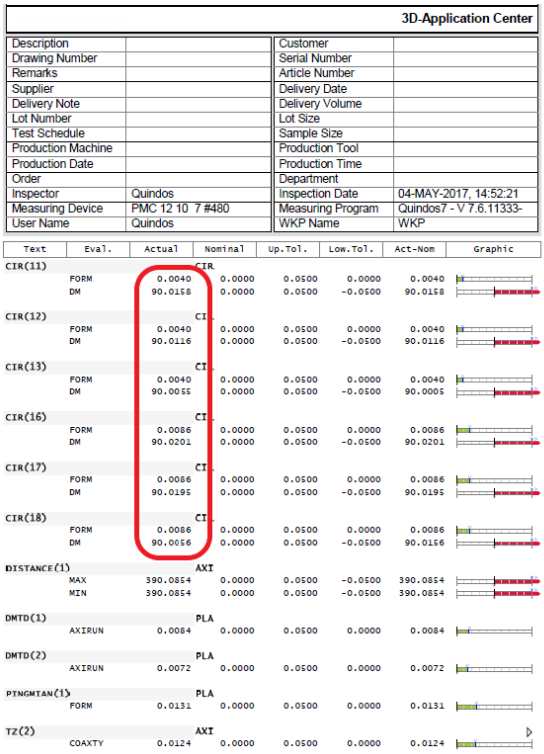

3D-Application Center

Description		Customer	
Drawing Number		Serial Number	
Remarks		Article Number	
Supplier		Delivery Date	
Delivery Note		Delivery Volume	
Lot Number		Lot Size	
Test Schedule		Sample Size	
Production Machine		Production Tool	
Production Date		Production Time	
Order		Department	
Inspector	Quindos	Inspection Date	04-MAY-2017, 14:52:21
Measuring Device	PMC 12 10 7 #480	Measuring Program	Quindos7 - V 7.6.11333-
User Name	Quindos	WKP Name	WKP

Text	Eval.	Actual	Nominal	Up.Tol.	Low.Tol.	Act-Nom	Graphic
CIR(11)			CIR				
	FORM	0.0040	0.0000	0.0500	0.0000	0.0040	
	DM	90.0158	0.0000	0.0500	-0.0500	90.0158	
CIR(12)			CI				
	FORM	0.0040	0.0000	0.0500	0.0000	0.0040	
	DM	90.0116	0.0000	0.0500	-0.0500	90.0116	
CIR(13)			CI				
	FORM	0.0040	0.0000	0.0500	0.0000	0.0040	
	DM	90.0055	0.0000	0.0500	-0.0500	90.0055	
CIR(16)			CI				
	FORM	0.0086	0.0000	0.0500	0.0000	0.0086	
	DM	90.0201	0.0000	0.0500	-0.0500	90.0201	
CIR(17)			CI				
	FORM	0.0086	0.0000	0.0500	0.0000	0.0086	
	DM	90.0195	0.0000	0.0500	-0.0500	90.0195	
CIR(18)			CI				
	FORM	0.0086	0.0000	0.0500	0.0000	0.0086	
	DM	90.0056	0.0000	0.0500	-0.0500	90.0156	
DISTANCE(1)			AXI				
	MAX	390.0854	0.0000	0.0500	-0.0500	390.0854	
	MIN	390.0854	0.0000	0.0500	-0.0500	390.0854	
DMTD(1)			PLA				
	AXIRUN	0.0084	0.0000	0.0500	0.0000	0.0084	
DMTD(2)			PLA				
	AXIRUN	0.0072	0.0000	0.0500	0.0000	0.0072	
PINGMIAN(1)			PLA				
	FORM	0.0131	0.0000	0.0500	0.0000	0.0131	
TZ(2)			AXI				
	COAXTY	0.0124	0.0000	0.0500	0.0000	0.0124	

Figure 5. The test data of part (length/diameter=20:1)

According to Figure 1, Figure 4, Eq.7 and Table 1, a comprehensive analysis is carried out. The test parts in Figures 1 and 4 is fixtured through surface bonding and coaxial rotation. Both Eq.7 and Table 1 show that the data measured by CIR (11), CIR (12) and CIR (13) are the error values of the 3 times excircle measurement at the B end of the workpiece, and the data measured by CIR (16), CIR (17) and CIR (18) are the error values of the 3 times excircle measurement at the A end of the workpiece. The precision range after data discovery and processing ranges from large to small. The main reason is that the fixture and workpiece will have an adaptive process through continuous grinding. This adaptive process is mainly manifested in the fact that with the grinding of the workpiece, the faint change between the workpiece and the fixture, the fixture and the machine tool becomes smaller and smaller. Then, through the comprehensive analysis of the two test errors, the final test accuracy error is about 2%. This shows that the accuracy model reflected by the two test conclusions can basically predict the machining accuracy of tooling and fixture.

4. Conclusion

Through the actual ultra-precision machining of thin-walled parts, it can be found that the accuracy of tooling and fixture will affect the machining quality of the whole part during the machining processes. In order to explain this phenomenon, we derive the plane error variation model and the cylinder error variation model based on the small displacement torsor (SDT) theory, and make theoretical analysis by combining the error variation matrices of the two models. The analysis process is mainly under two different machining dimensions, different machining feed and different machining clamping methods, and the final test accuracy deviation is within 2%. It's shown that it is feasible to analyse the weight ratio of plane error variation and cylindricity error variation, thus researching the machining accuracy of the whole thin-walled part. Mastering this kind of

aspect can be combined with the actual theoretical analysis to find out what kind of accuracy has the greatest impact.

Acknowledgement

This project is supported by the National Key Research and Development Program of China（2018YFB2000502）.

References

[1] Wang T, Cheng J, Liu H, Chen M, Wu C, and Su D 2019 Ultra-precision grinding machine design and application in grinding the thin-walled complex component with small ball-end diamond wheel *Int J Adv Manuf Tech* **101** 2097–2110

[2] Sosa A D, Echeverría M D, Moncada O J and Sikora J A 2007 Residual stresses, distortion and surface roughness produced by grinding thin wall ductile iron plates *Int J Mach Tool Manu* **47**(2) 229-235

[3] Huan J and Ma W 2010 Method for graphically evaluating the workpiece's contour error in non-circular grinding process *Int J Adv Manuf Tech* **46**(1-4) 117-121

[4] Fu G, Fu J, Shen H, Sha J, and Xu Y 2016 Numerical solution of simultaneous equations based geometric error compensation for CNC machine tools with workpiece model reconstruction *Int J Adv Manuf Tech* **86** 2265–2278

[5] Skoblo T S, Romaniuk S P, Sidashenko A I, Garkusha I E, Taran V S, Taran A V and Pilgui N N 2018 Strengthening Method for Thin-Walled Knives with Multi-Layer Nanocoatings and Quality Assessment by Non-Destructive Method *J Adv Micro Rese* **13**(3) 333-338